EBioMedicine 41 (2019) 370–383

Contents lists available at ScienceDirect

EBioMedicine

journal homepage: www.ebiomedicine.com

EBioMedicine
Published by THE LANCET

Oxidized ATM-mediated glycolysis enhancement in breast cancer-associated fibroblasts contributes to tumor invasion through lactate as metabolic coupling

Kexin Sun [a,1], Shifu Tang [a,b,c,1], Yixuan Hou [a,d], Lei Xi [a], Yanlin Chen [a], Jiali Yin [a], Meixi Peng [a], Maojia Zhao [a], Xiaojiang Cui [e], Manran Liu [a,*]

[a] Key Laboratory of Laboratory Medical Diagnostics, Chinese Ministry of Education, Chongqing Medical University, Chongqing 400016, China
[b] Department of Laboratory Medicine, Liuzhou Traditional Chinese Medical Hospital, Liuzhou 545001, Guangxi, China
[c] Department of Laboratory Medicine, The Third Affiliated Hospital of Guangxi University of Chinese Medicine, Liuzhou 545001, Guangxi, China
[d] Experimental Teaching Center of Basic Medicine Science, Chongqing Medical University, Chongqing 400016, China
[e] Department of Surgery, Samuel Oschin Comprehensive Cancer Institute, Cedars-Sinai Medical Center, Los Angeles, CA 91006, USA

ARTICLE INFO

Article history:
Received 25 September 2018
Received in revised form 31 January 2019
Accepted 13 February 2019
Available online 22 February 2019

Keywords:
CAFs
Oxidized-ATM
Hypoxia
GLUT1
PKM2(PYKM2)

ABSTRACT

Background: Cancer-associated fibroblasts (CAFs) are the predominant residents in the breast tumor microenvironment. In our work, we found activation of DNA damage-independent ATM (oxidized ATM), enhanced glycolysis and aberrant metabolism-associated gene expressions in breast CAFs. Nevertheless, whether and how oxidized ATM regulates the glycolytic activity of CAFs keep in unveil. Recently, a reverse Warburg effect was observed in tumor tissues, in which host cells (such as CAFs, PSCs) in the tumor microenvironment have been found to "fuel" the cancer cells via metabolites transfer. However, the molecular mechanisms of the metabolites from stromal cells playing a role to the progression of cancer cells remain to be determined.
Methods: Oxidized ATM activation in stromal CAFs was assessed by western blotting and immunofluorescence. The increased glycolytic ability of CAFs was validated by measurements of OCR and ECAR and detections of glucose consumption and lactate production. Kinase assay and western blotting were performed to confirm the phosphorylation of GLUT1. The membrane location of phosphorylated GLUT1 was determined by biotin pull-down assay and immunofluorescence staining. The regulation of PKM2 through oxidized ATM was evaluated by western blots. In addition, the impact of lactate derived from hypoxic CAFs on cancer cell invasion was investigated both in vitro (transwell assays, western blots) and in vivo (orthotopic xenografts).
Findings: Hypoxia-induced oxidized ATM promotes glycolytic activity of CAFs by phosphorylating GLUT1 at S490 and increasing PKM2 expression. Moreover, lactate derived from hypoxic CAFs, acting as a metabolic coupling between CAFs and breast cancer cells, promotes breast cancer cell invasion by activating the TGFβ1/p38 MAPK/MMP2/9 signaling axis and fueling the mitochondrial activity in cancer cells.
Interpretation: Our work shows that oxidized ATM-mediated glycolysis enhancement in hypoxic stromal fibroblasts plays an essential role in cancer cell invasion and metastasis and may implicate oxidized ATM as a target for breast tumor treatment.
Fund: This research was supported by National Natural Science Foundation of China.
© 2019 The Authors. Published by Elsevier B.V. This is an open access article under the CC BY-NC-ND license (http://creativecommons.org/licenses/by-nc-nd/4.0/).

Abbreviations: ATM, ataxia-telangiectasia mutated protein kinase; DSB, double-strand break; PSCs, pancreatic stellate cells; CAFs, cancer-associated fibroblasts; NFs, normal fibroblasts; GLUT1, glucose transporter 1; PKM2 (PYKM2), pyruvate kinase M2; ROS, reactive oxygen species; HnRNP, heterogeneous nuclear ribonucleoprotein; TCA, mitochondrial tricarboxylic acid; hTERT, human telomerase reverse transcriptase gene; shRNA, short hairpin RNA; CM, conditioned medium; ECM, extracellular matrix; TEM, Transmission Electron Microscope; CCD, Charge Coupled Device; 2-DG, 2-Deoxy-Glucose; CHC, α-cyano-4-hydroxycinnamic acid; H&E, hematoxylin and eosin; IF, immunofluorescence; LC-MS/MS, liquid chromatography-tandem mass spectrometry; NAC, N-Acetylcysteine; MCT4, monocarboxylate transporter4; MCT1, monocarboxylate transporter1; OXPHOS, oxidative phosphorylation; OCR, oxygen-consumption rate; ECAR, extracellular acidification rate; FN, fibronectin; α –SMA, α-smooth muscle actin; FAP, fibroblast activation protein.

* Corresponding author at: Key Laboratory of Laboratory Medical Diagnostics, Chinese Ministry of Education, Chongqing Medical University, No.1, Yi-Xue-Yuan Road, Yu-zhong District, Chongqing 400016, China.
E-mail address: manranliu@cqmu.edu.cn (M. Liu).
[1] Kexin Sun and Shifu Tang contributed equally to this work.

https://doi.org/10.1016/j.ebiom.2019.02.025
2352-3964/© 2019 The Authors. Published by Elsevier B.V. This is an open access article under the CC BY-NC-ND license (http://creativecommons.org/licenses/by-nc-nd/4.0/).

Research in context

Evidence before this study

Many studies verified that CAFs play indispensable roles in cancer progression including tumor growth, invasion, and metastasis directly or indirectly through paracrine pathways. Recently, the glucose metabolism alterations (Warburg effect) was found as a new feature of CAFs. Nevertheless, the underlying mechanism of glycolysis in CAFs and its role in promoting the progression and development of tumors still remain to be researched.

Added value of this study

In this study, we found the enhanced glycolysis in CAFs compared to NFs and oxidized ATM can promote the glycolysis in breast CAF under hypoxia. To investigate the effect of oxidized ATM on glycolysis enhancement of CAFs and the underlying mechanism. We discovered that hypoxia-induced oxidized ATM induces glycolysis of CAFs by promoting the GLUT1 membrane translocation through the phosphorylation of GLUT1 at S490. In addition, the PKM2 expression in CAFs was up-regulated by the activation of ATM through PI3K/AKT signaling pathway. Moreover, the invasion of the breast cancer cells (MDA-MB-231, BT-549) was accelerated by the energy metabolic coupling mediator-lactate produced by CAFs. Besides, lactate between CAFs (released by MCT4) and tumor cells (absorbed via MCT1) may accelerate tumor cell invasion via activation of TGFβ1/p38 MAPK/MMP2/9 signaling and boost of mitochondrial activity in tumor cells. In summary, the influence of oxidized ATM on glycolysis of CAFs and the underlying mechanism about the pro-invasion impact of CAFs were investigated.

Implications of all the available evidence

Our findings highlighted a novel mechanism by which stromal fibroblasts fuel tumor invasion through metabolic symbiosis and may indicate a new strategy targeting oxidized-ATM for breast cancer therapy.

1. Introduction

Cancer-associated fibroblasts (CAFs), namely activated fibroblasts, are the predominant residents in the breast tumor microenvironment [1]. CAFs play indispensable roles in cancer progression including tumor growth, invasion, and metastasis directly or indirectly through paracrine pathways [2]. Growing evidence show that tumor cells have altered metabolic patterns to meet both catabolic ATP producing and anabolic biomass synthesizing demands. For example, triple negative breast cancer (TNBC) cells mainly depend on OxPhos whereas MCF-7 cells perform on OxPhos and glycolysis, and some cancer cells (e.g. CT26, glioma C6) are relied on glycolysis [3]. Recently, metabolism of non-tumor cells in tumor microenvironment was reported, and the enhanced glycolysis and reduced oxidative phosphorylation has been characterized as a feature of CAFs [4]. Hypoxia is a common feature in most tumors as a result of poor blood supply [5]. Recently, hypoxia has been shown to promote the glycolysis of cancer cells and causes cellular oxidative stress through reactive oxygen species (ROS) generation [6]. To date, whether and how hypoxia promotes the glycolytic activity in CAFs is not fully understood.

The ataxia-telangiectasia mutated protein kinase (ATM) controls cellular response to DNA damage and maintenance of cellular homeostasis. For example, ATM can phosphorylate the downstream checkpoint kinase CHK2 and checkpoint proteins RAD17 and RAD9, thereby acting as an important regulator of cell cycle progression [7,8]. ATM-mediated phosphorylation of DYRK2 and ATF2 plays critical roles in stress-induced genotoxicity [9] and DNA damage response [10], respectively. All these findings demonstrate a DNA double-strand break (DSB)-dependent ATM activation. On the other hand, ATM could also be activated by oxidative stress (such as ROS), which is independent of DNA damage [11], this kind of ATM is called oxidized ATM or DNA double-strand breaks (DSBs)-independent ATM. A growing number of studies have shown that ATM can be activated in the absence of DSB to regulate cell proliferation [12,13], and the activation of oxidized ATM has been found to regulate translocation of glucose transporter 4 in mouse muscle cells [14]. In addition, as a redox sensor, ATM can be oxidized by mitochondria-derived ROS under hypoxia and functions as a regulator of p53 signaling and glucose metabolism in mouse embryonic fibroblasts [15]. In our work, we found an aberrant ATM signaling and sets of the altered metabolism-associated genes in breast CAFs compared with normal fibroblasts (NFs) [16]. These studies suggest oxidized ATM probably involves in the increased glycolytic activity in hypoxic CAFs. Nevertheless, whether and how oxidized ATM regulates the increased glycolytic activity of hypoxic CAFs remains to be determined.

Energy metabolism is regulated by a series of genes including glucose transporter 1 (GLUT1) and several glycolysis related kinase such as pyruvate kinase M2 (PKM2) and lactate dehydrogenase A (LDHA). GLUT1 contributes to cancer cell metabolism reprogramming through transporting glucose from extracellular matrix for glycolysis, and the subcellular localization of GLUT1 may be a key regulator of glucose uptake [17]. Posttranslational modifications such as phosphorylation may influence the subcellular localization of GLUT1 in muscle skeletal cells [18]. Whether phosphorylation of GLUT1 regulates increased glycolytic activity in CAFs is unknown. It has been shown that PKM2 expression is often elevated in many tumor cells, and plays a vital role in glycolysis by dephosphorylating phosphoenolpyruvate to pyruvate at the final rate-limiting step [19]. PKM2 can be transcriptionally activated by heterogeneous nuclear ribonucleoprotein (hnRNP) family members and the oncogenic transcription factor c-Myc [20]. Hypoxia can also activate the PKM2 promoter by down-regulating Sp3, thereby removing the associated transcriptional suppressor to induce PKM2 expression [21]. However, whether oxidized ATM, which is activated by hypoxia, regulates PKM2 expression or activation and consequently increased glycolytic activity is unclear.

Recently, a reverse Warburg effect was observed in tumor tissues, in which host cells in the tumor microenvironment have been found to "fuel" tumor cell growth via energy transfer. For example, tumor cells can take up the metabolites lactate and pyruvate from the caveolin-1 deficient stromal fibroblasts to use them as energy fuels in mitochondrial tricarboxylic acid (TCA) cycle to enhance tumor proliferation [4]. The ketone bodies (e.g. BDH1 and HMGCS2) supplied by catabolic fibroblasts can increase mitochondrial mass in carcinoma cells, thus enhancing tumor cell growth and invasion capacity [22]. Increased glutamines from fibroblasts potentiate survival and tamoxifen-resistance in breast epithelial cancer cells [23]. However, the detail molecular mechanisms of metabolites from stromal cells to fuel tumor cell growth and invasion keep in unveil. Recently, Dr. Dong Chul Lee and his colleagues reveal that lactate can bind as stabilizer to the NDRG3 protein to mediate hypoxia-induced activation of Raf-ERK pathway, thereby promoting angiogenesis and cell growth [24].

In this study, we investigated the effect of oxidized ATM on the increased glycolytic activity of CAFs and the underlying mechanism. We found that hypoxia-induced oxidized ATM induces glycolytic activity of CAFs by phosphorylating GLUT1 at S490 and increasing PKM2 expression. Moreover, the energy metabolic coupling mediator lactate, produced by CAFs, promotes breast cancer cell invasion by activating the TGFβ1/p38 MAPK/MMP2/9 signaling axis and increase mitochondrial activity in tumor cells. These findings reveal a novel role of CAFs in pro-invasion breast tumors, and may implicate an oxidative ATM-targeting strategy for breast tumor treatment.

2. Materials and methods

2.1. Cell culture

CAFs and NFs were isolated from breast tumor tissues and their paired normal tissues and identified with CAF-related biomarkers, respectively; and were immortalized by human telomerase reverse transcriptase gene (hTERT) as described previously [16,25]. NFs and CAFs were cultured in DMEM (C11995500BT, Gibco) with 10% FBS (10099-144, Gibco, Austrlia); Human breast cancer cells MDA-MB-231 and BT-549 were maintained in RPMI-1640 medium (C11875500BT, Gibco) with 10% FBS at 37 °C in a tri-gas incubator containing 5% CO_2 under normoxic (21% O_2) or hypoxic (1% O_2 and 94% N_2) condition. The genotyping of these breast cancer cells shared >94% of the STR loci with the ATCC original clones by STR identification (Genewiz, Suzhou).

2.2. RNA interference, plasmids and engineered fibroblasts

All the synthetic short hairpin RNA (shRNA) oligonucleotides, lentivirus expression vector of shRNA against ATM, GLUT1, PKM2, MCT4, MCT1 and the control shRNA were purchased from GenePharma (Shanghai, China). The sequences of shRNA are listed in Supplementary Table 1. The wild type GLUT1 S490 (FHPLGADSQV; WT), mutant GLUT1 S490A (from FHPLGADSQV to FHPLGADAQV to lead a hypophosphorylated GLUT1) constructs were generated by GenePharma (Shanghai, China) and inserted into pcDNA-Flag tagged plasmid to get pcDNA-Flag-GLUT1 (WT) and pcDNA-Flag-GLUT1 mutant (S490A). The pcDNA3-Flag-ATM construct was obtained from Addgene.

The engineered CAFs with a stable expression of shATM, shGLUT1, shPKM2, shMCT4 and the breast cancer cells (MDA-MB-231 and BT-549) with a stable expression of shMCT1 were established using the lentivirus infection as described elsewhere. In order to establish the engineered GLUT1 WT- and GLUT1 mutant-CAFs, the endogenous *glut1* of CAFs was knocked down by GLUT1 shRNA (named CAF/*glut1* KD). The ectopic WT, mutant GLUT1 S490A was then transfected into CAFs to acquire the engineered CAFs stably expressing WT (CAF/ecto-WT) or mutant GLUT1 (CAF/ecto-S490A).

2.3. Immunohistochemistry staining (IHC) and immunofluorescence (IF)

Tumor tissues were fixed with 4% paraformaldehyde and then sectioned into 4 μm of sections. IHC was performed according to protocols of the manufacturor. The sections were incubated with rabbit anti-MMP2, MMP9, p-ATM, GLUT1, PKM2 and TGFβ1 polyclonal antibody (1:200, Bioworld) overnight at 4 °C. Then, the sections were sequentially incubated with polyperoxidase-anti-rabbit IgG (ZSBiO) for 30 min at 37 °C, then stained with diaminobenizidine.

Immunofluorescence staining was done following the standard protocol as described previously [16]. The primary antibodies specifically against FN (ab23750, abcam,1:200), α-SMA (ab5694, abcam,1:200), ATM (ab47575, abcam, 1:200), p-ATM (ab19304, abcam, 1:200), γH2AX (5883, CST, 1:200), 53BP1 (ab175933, abcam, 1:200), GLUT1 (ab14683, abcam, 1:200), PKM2 (sc365684, Santa Cruz, 1:150) were used. Normal rabbit IgG was the negative control. IHC and IF images were captured using a Nikon Eclipse 80i microscope (Tokyo, Japan).

2.4. Western blotting analysis

Western blotting analysis was performed as described previously [11]. Briefly, total cell proteins were obtained using RIPA lysis buffer (P0013B, Beyotime, China), quantified with the BCA protein assay kit (P0012, Beyotime). 50 μg of total proteins were separately electrophoresed in 8%–12% SDS-PAGE gel, subsequently incubated with appropriate primary antibodies as followings: FN (ab23750, abcam,1:1000), FAP (ab53066, abcam,1:1000), α-SMA (ab5694, abcam,1:1000), ATM (2873, CST, 1:1000), p-ATM (5883, CST, 1:1000), γH2AX (9718, CST, 1:1000), CHK2-T68 (ab32148, abcam, 1:1000), Na^+/K^+ ATPase (ab58457, abcam, 1:800), Hsp90 (ab13492, abcam, 1:800), AKT (4685, CST, 1:1000), p-AKT (12694 s, CST, 1:1000), GLUT1 (ab14683, abcam, 1:500), p-ST/Q (6966 s, CST, 1:1000), PKM2 (sc365684, Santa Cruz, 1:500), MCT4 (ab74109,1:1000), MCT1 (ab90582,1:1000) TGFβ1 (ab675195, abcam, 1:1000), P38 (bs4635, bioworld, 1:1000), p-P38 (bs3566, bioworld, 1:1000), MMP2 (ab92538, abcam, 1:800), and MMP9 (ab76003, abcam, 1:800), GLUT3 (ab41525,1:800), HK2 (ab104836,1:800), HPI (ab86950,1:1000), LDHA (ab101562,1:1000). The appropriate horseradish peroxidase (HRP)-conjugated anti-mouse or rabbit IgG (ZSGBBIO, China) was used as secondary antibodies. The protein bands were visualized using the enhanced chemiluminescence system (Amersham Pharmacia Biotech, Tokyo, Japan).

2.5. Immunoprecipitation-Western blotting (IP-WB) assays

Co-immunoprecipitation was performed as previously described [26]. The cell lysates were pre-treated with Protein A/G Magnetic Beads (B23202, Selleckchem, TX, USA), and then immunoprecipitated with 2 μg of p-ST/Q (6966 s, CST, Boston) and 20 μl Protein A/G Magnetic Beads at 4 °C overnight. After washing with lysis buffer carefully, the protein complexes were released from the beads by boiling in 2× loading buffer and subjected to Western blotting assays.

2.6. Detection of cell membrane GLUT1 with biotinylation of cell surface proteins

In brief, CAFs were cultured in growth medium to around 85% confluence, and then cultured under the normoxic or hypoxia condition in FBS-free medium for 8 h with or without Ku60019 treatment. After washing with pre-cooled PBS, membrane proteins form cells were labeled with 1 Mm EZ-Link Biotin (Thermo Scientific) on ice for 30 min followed by quenched with biotin quench solution (250 mm Trizma Base). Cells were collected with Biotin Lysis Buffer and centrifuged at 14000 r/min for 10 min to obtain the supernatants containing membrane proteins labeled with biotin. Streptavidin beads (Thermo Scientific) were used to immunoprecipitate the supernatants for 15 min. After washing with TBS and boiling with sample buffer, the supernatants were used to western blotting. Na+/K + -ATPase was used as a loading control for cell surface proteins.

2.7. Determination of ATM kinase activity by monitoring ADP formation

HEK293 cells were transfected with pcDNA3-Flag-ATM, pcDNA3-Flag-GLUT1 WT or pcDNA3-Flag-GLUT1 S490A construct, respectively. The HEK293 cells transfected with GLUT1 were regularly cultured in 21% O_2. The HEK293 cells transfected with ATM were cultured in the hypoxic condition combined with or without 5 μM KU60019 treatment for 8 h. Flag-ATM and Flag-Cortactin were immunopurified from the extracts with Anti-FLAG® M2 Magnetic Beads (M8823, Sigma). Kinase reactions were conducted by incubating purified ATM with purified GLUT1 WT or S490A in kinase reaction solution in a 96-well plate according to the protocol of Universal Kinase Assay Kit (Fluorometric) (abcam, ab138879). Then 20 μl of ADP Sensor Buffer and 10 μl of ADP Sensor were added into each well and the reaction mixture was incubated in dark at room temperature for 30 min. After reaction, the fluorescence intensity of ADP products was detected with a microplate fluorescence reader (BioTek, flx800) at Ex/Em = 540/590 nm. Proteins were immunoblotted with the antibodies to GLUT1 and p-GLUT1.

2.8. Preparation of conditioned medium (CM)

CAFs or the engineering CAFs (2.0×10^6) were seeded into a 6 well plate in growth medium. After removing the growth medium, DMEM (2 ml) with 0.5% FBS was added to further culture in hypoxia condition

for 8 h, and the supernatant was collected and centrifuged to obtain conditioned medium.

2.9. Cell migration and invasion assay

Cell migration and invasion were measured by Boyden chamber assay as described previously [25]. Briefly, MDA-MB-231 or BT-549 cells (2×10^4) suspended in 200 μl serum-free medium (CM or CM with exogenous lactate) were seeded into the wells of 8 μm-pore Boyden chambers (Millipore, Darmstadt, Germany) coated with (for cell invasion assay) or without (for cell migration assay) ECM (1:7.5) (Sigma, St. Louis, MO). Medium with FBS was added into the lower chamber. Cells can invade toward medium in the lower chamber, and the invaded cells on the opposite side of the filter were stained with crystal violet in methanol and counted after incubation for 8 h. All the experiments were repeated in three times.

2.10. Measurement of glucose consumption, lactate production

The glucose consumption and lactate production were measured using the Glucose Assay Kit and Lactate Assay Kit according to the manufacturer's instructions (Jiancheng Bioengineering Institute, Nanjing, China). Briefly, 4×10^5 of NFs, CAFs, engineered CAFs (CAF/ecto-WT, CAF/ecto-S490A, CAF/sh-ATM, CAF/sh-PKM2, CAF/sh-MCT4, and CAF/sh-Ctrl) and their control cells were plated in 12-well plates. Cell culture and treatments in the experiments were described in detail in the figure legends. At the end of the experiments, the samples (supernatant or cell lysates) were prepared and glucose probe, glucose enzyme mix (for glucose assay) or lactate enzyme mix, lactate substrate mix (for lactate assay) were added to the samples. After incubating at room temperature for 30 min, the absorbance (OD 505 nm for glucose assay) or optical density (OD 530 nm for lactate assay) were measured with a microplate reader (BioTek, Winooski, Vermont, USA), separately. The glucose consumption and lactate production were normalized by cell numbers.

2.11. Mitochondrial detection by transmission electron microscopy (TEM)

NFs and CAFs were harvested and fixed in glutaraldehyde and 1% osmium tetroxide for 2 h at 4 °C, separately. After being dehydrated in ethanol and acetone, the cells were embedded in epoxy resin and polymerized at 60 °C. Ultrathin sections with the thickness of 60 nm were prepared and stained with uranyl acetate and lead citrate. Slides were observed under TEM (Hitachi-7500, Japan) and photographed using a CCD camera (Gatan-780CCD, USA).

2.12. Detection of intracellular reactive oxygen species (ROS)

The intracellular ROS levels of stromal fibroblasts were measured by Reactive Oxygen Species Assay Kit (S0033, Beyotime) according to the manufacturer's instructions. Briefly, CAFs were cultured in normoxic or hypoxic conditions for 8 h with or without 1 mM NAC. Then, 10 μM of DCFH-DA was added to cells and incubated continually for 30 min. Total cell lysate was obtained by lysing with RIPA buffer (P0013B, Beyotime), and fluorescent compound was scanned at excitation and emission wavelengths of 485 and 535 nm by using Cary Eclipse (Agilent) for determination.

2.13. The measurements of OCR and ECAR

The cellular OXPHOS and glycolysis were detected by monitoring the OCR (oxygen-consumption rate) and ECAR (extracellular acidification rate) with the Seahorse Bioscience Extracellular Flux Analyzer (Seahorse Bioscience Inc.). Briefly, 2×10^4 cells were seeded in 24-well plates matched for XF24. Before measurements, cells were washed and then incubated with unbuffered media in a CO_2 free incubator for 45 min. The detection of OCR was performed in XF Base Media and the following inhibitors were added: oligomycin (2 μM), carbonyl cyanide 4-(trifluoromethoxy) phenylhydrazone (FCCP) (1.5 μM) and rotenone/antimycin A (0.5 μM/1 μM). The detection of ECAR was performed in XF Base Media and the following inhibitors were added: Rotenone/Antimycin A (0.5 μM/1 μM) and 2-deoxy-glucose (20 mM). Measuring OCR before and after addition of oligomycin, correlates to the mitochondrial respiration from ATP production, then the oligomycin-sensitive OCR (OxPhos OCR) was acquired. Measuring ECAR before and after addition of 2-deoxy-glucose (2-DG), confirming the ECAR produced in the experiment is due to glycolysis, then the glycolytic ECAR was obtained. OCR and ECAR were normalized according to cell number (1×10^4).

2.14. Detection of mitochondrial membrane potential

The mitochondrial membrane potential of NFs and CAFs were measured using the JC-1 kit (C2006; Beyotime) according to the manufacturer's protocols. Cells (1×10^6) were seeded and grow overnight, then stained with JC-1 dye, the mean orange-red fluorescence (FL-2 channel) were recorded and quantified by flow cytometry (BD Biosciences).

2.15. Orthotopic xenografts and lung metastasis analysis

Animal experiments were authorized by the animal use committees of Chongqing Medical University. MDA-MB-231 cells (1×10^6) mixed with control CAFs (CAF/Ctrl) or engineered CAFs (1×10^6) in 200 μl of PBS:Matrigel at a 1:1 ratio were subcutaneously injected into 4-week-old female nude mice. The two axes of tumor were assessed by caliper measurements every three days to calculate the tumor volume (($L \times W^2$)/2). When the tumor was around 50 mm^3, the mice implanted with MDA-MB-231 and CAF/sh-Ctrl were intraperitoneally administered with 2-DG (2-Deoxy-Glucose, Sigma, 500 mg/kg, three times a week.) or CHC (α-cyano-4-hydroxycinnamic acid, Sigma, 25 μmol in 200 μl, daily); the mice injected with MDA-MB-231 and CAF/sh-ATM were intraperitoneally administered with lactate (Sigma, 100 μmol in 200 μl, daily). At the end of animal experiments, mouse lungs were serially sectioned into 5 μm sections and prepared for hematoxylin and eosin (H&E) staining for subsequent blinded evaluation of metastases in the lungs.

2.16. Ethics statement

Animal experiments were permitted by the animal use committees of Chongqing Medical University. All animal work was conducted in accordance with an approved protocol and carried out according to the institutional animal welfare guidelines of the Chongqing Medical University.

2.17. Statistical analysis

Statistical significance was determined using SPSS 19.0 software. The results are shown as means ± SD. Multiple groups were analyzed using ANOVA followed by the Student-Newman-Keuls multiple comparison test, and single comparison between two groups was analyzed using Student's *t*-test. A *P*-value <.05 was considered to be statistically significant.

3. Results

1. There are an aberrant energy metabolism-associated gene expression profile and increased glycolytic activity in breast CAFs.

Our previous studies showed the different biological characteristics and global gene expression profiles between breast CAFs and NFs [16]. Using bioinformatics analysis, we found a set of altered genes associated with energy metabolism in CAFs (Fig. 1a). CAFs and their paired NFs

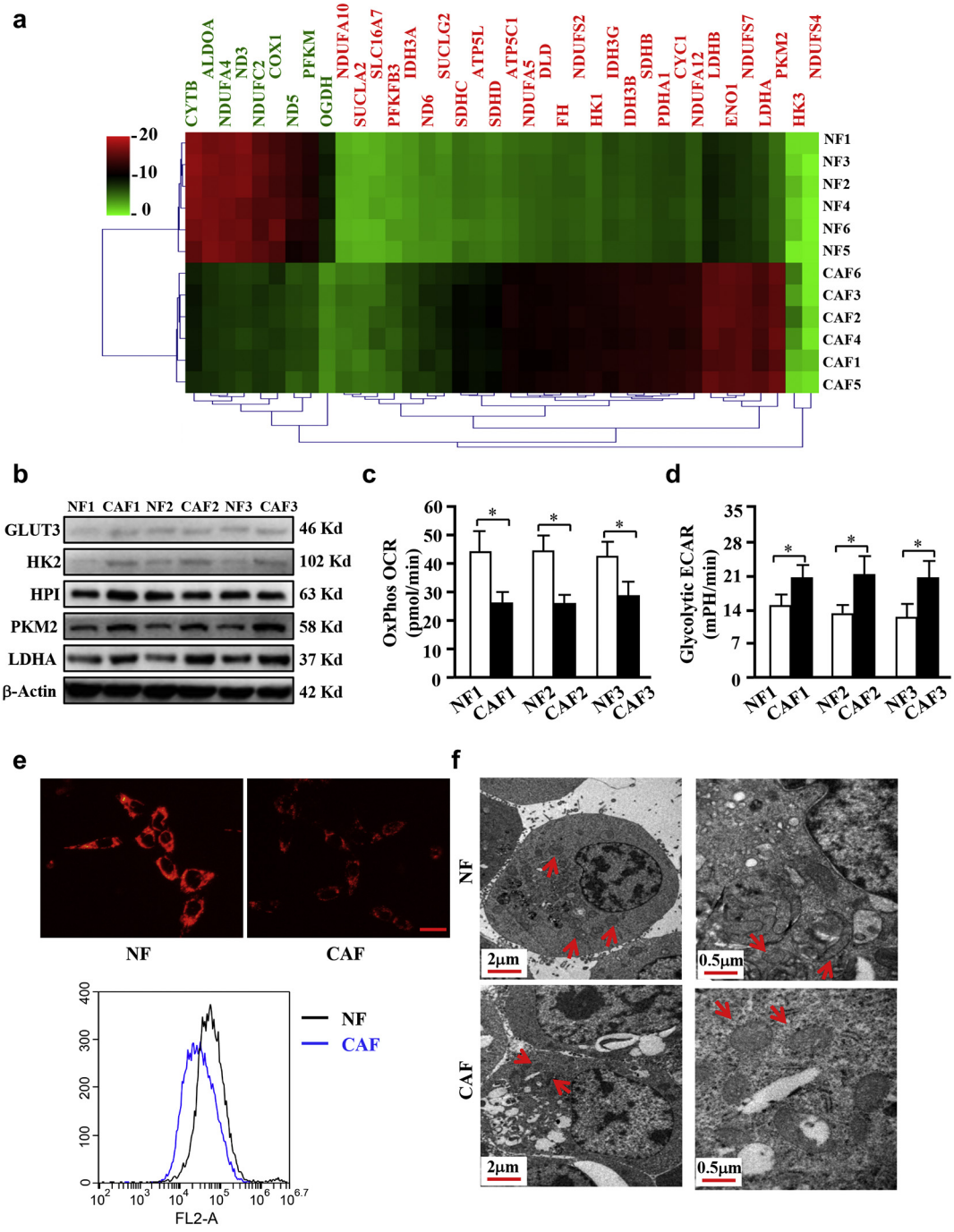

Fig. 1. Higher glycolysis phenotype in CAFs compared with NFs. a. Heat-Map of the dysregulated genes involved in energy metabolism in 6 paired breast CAFs and NFs detected by Agilent mRNA microarrays. Red or green indicates the up-regulated or down-regulated genes, respectively (Fold changes>1.8; $P < .05$, CAFs vs NFs). b. The protein levels of some metabolism-related genes were detected with the indicated antibodies. β-Actin is the loading control. c-d. The OCR from OxPhos (c) and ECAR from glycolysis (d) of NFs and CAFs were detected (*, CAFs vs NFs, $P < .05$, Student's *t*-test). e. JC-1 staining was used to detect mitochondrial membrane potential of NFs and CAFs, the quantification was detected by flow cytometer. Scale bar, 50 μm. f. Graphs detected by transmission electron microscope show the numbers of mitochondrial and mitochondrial crista in NFs and CAFs. Red arrows indicate the numbers of mitochondrial (left panels, scale bar, 2 μm) or mitochondrial crista (right panels, scale bar, 0.5 μm).

were isolated from breast tissue. CAFs was identified with fibronectin (FN), which is the biomarker of fibroblasts, and CAFs-selective biomarkers including α-smooth muscle actin(α -SMA)and fibroblast activation protein(FAP)through Q-PCR (Fig. S1a). The expression changes of these biomarkers were reproved by western blotting in 3 paired of NFs and CAFs (Fig. S1b). FN was universally expressed in NFs and CAFs and the expression of α -SMA was high in CAFs (Fig. S1c). These data demonstrated that the purified CAFs were successfully acquired from tumor tissue. Higher levels of PKM2 and LDHA were detected in CAFs by cDNA microarray and confirmed again by western blotting in another three pairs of NFs and CAFs (Fig. 1b). Some metabolism genes such as GLUT-3, HK2 and HPI were reported abnormal expressed in some cancer cells [27], these genes were also detected in in NFs and CAFs. As shown in Fig. 1b, the levels of GLUT-3, HK2 were very low in NFs and CAFs, although a litter bitter higher GLUT-3 and HK2 in CAFs compared to NFs, indicating that GLUT3 and HK2 are not the dominate factors in the glycolysis process of CAFs. The expression of HPI has no significant difference between CAFs and NFs, it was not considered as

a differential gene. To experimentally test the glycolytic activity in CAFs, oxygen-consumption rate (OCR) from OxPhos and extracellular acidification rate (ECAR) from glycolysis were examined using primary NFs and CAFs. Indeed, lower levels of OxPhos OCR (Fig. 1c) and higher levels of glycolytic ECAR (Fig. 1d) were detected in CAFs than in NFs. Furthermore, weaker mitochondrial membrane potentials were also detected in CAFs compared with NFs (Fig. 1e). Consistently, less mitochondria (Fig. 1f, left panel) and reduced mitochondria crista (Fig. 1f, right panel) were observed by transmission electron microscopy (TEM) in CAFs than in NFs. To further investigate the glycolytic activities of CAFs, immortalized breast CAFs were cultured in different O_2 concentrations for 3 h. A hypoxia-dependent glycolysis was corroborated by testing glucose consumption and lactate generation (Fig. S2a). Similarly, a time-dependent glycolysis induced by hypoxia was also observed in CAFs (Fig. S2b). These data demonstrate the enhanced glycolysis is in breast CAFs.

2. Hypoxia stimulates the activation of DSB-independent oxidized ATM kinase to promote glycolysis in CAFs.

Our previous study showed that aberrant ATM signaling may exist in CAFs [16]. Using primary fibroblasts isolated from breast tumors, we detected higher levels of phosphorylated ATM in CAFs (Fig. S2c). The activation of ATM (p-ATM) could be stimulated by hypoxia and maintained at a high level with no DNA damage at 8 h; and just a few of DNA damage appeared around 12 to 24 h in hypoxia, which evaluated by γH2AX and CHK2 (T68) proteins, two of known biomarkers of double-strand break (DSB) (Fig. 2a) (CAFs were then cultured in hypoxia around 8 h in subsequent experiments to avoid DSB), suggesting an DSB-independent ATM (or called oxidized ATM) activation in CAFs. In agreement with this result, the increased p-ATM was detected in cytoplasm rather than in nucleus by immunofluorescence staining in CAFs under hypoxia for 8 h (Fig. S2d). However, cisplatin (a DSB-induced chemical drug) treatment resulted in an obvious DNA damage-dependent ATM activation with enhanced γH2AX and CHK2 (T68) in CAFs (Fig. 2b). Consistently, nuclear 53BP1 and γH2AX (biomarkers of DSBs) were also observed in CAFs treated with cisplatin rather than in hypoxic CAFs (Fig. S2e). These data demonstrated that oxidized ATM is activated in a DSBs-independent manner in hypoxic CAFs. To explore whether oxidized ATM acts as a redox sensor [28] for hypoxia, CAFs were cultured in hypoxic conditions with or without antioxidant NAC for 8 h, cellular ROS levels were measured by DCF fluorescence detection. Hypoxia treatment could significantly increase ROS levels in CAFs, which were mitigated by antioxidant NAC (Fig. S2f). Correspondingly, p-ATM protein levels were enhanced in hypoxic condition but diminished by NAC, with no influence on the total ATM protein in CAFs (Fig. S2g), indicating that ATM protein may be oxidized and activated by ROS under hypoxia.

Accumulating evidence suggests that ATM has been involved in energy metabolism [28]. Next, we tested whether the oxidized ATM kinase contributes to glycolytic activity in CAFs. It was found that hypoxia-enhanced glucose consumption and lactate products were decreased by antioxidant NAC (Fig. S1h). To directly explore the effect of oxidized ATM on glycolysis in breast CAFs, an ATM specific inhibitor KU60019 was used. As expected, levels of p-ATM (s1981) were pronouncedly increased in hypoxic CAFs and apparently decreased in the presence of KU60019 (Fig. 2c left panel). Glycolytic activity was also significantly impaired by the ATM inhibitor KU60019 in hypoxic CAFs (Fig. 2c, middle and right panel). Knockdown of ATM in CAFs (Fig. 2d, left panel) led to a notably reduced glycolysis (Fig. 2d, middle and right panel). The enhanced glucose consumption and lactate generation were also detected in another 5 of primary hypoxic CAFs isolated from breast tumor tissues (Fig. 2e), and attenuated by KU60019 treatment (Fig. 2f). These data indicate that oxidized ATM promotes glycolytic activity in hypoxic breast CAFs.

3. GLUT1 is a phosphorylated target of oxidized ATM kinase in CAFs.

To understand the potential mechanisms of oxidized ATM in promoting glycolysis of hypoxic CAFs, quantitative phosphoproteome analysis was performed using high-resolution LC-MS/MS analysis. 1294 differential phosphosites in 615 proteins were identified in hypoxic CAFs, among which 113 sites in 33 proteins contains SQ or TQ motif, the potential phosphosites of oxidized ATM kinase (Supplemental Table 2). There are seven phosphorylated proteins involved in energy metabolism in hypoxic CAFs (Supplemental Table 3).

GLUT1, essential for glucose uptake in cells [29], is one of significantly changed phospho-protein in the phosphoproteome of CAFs. Serine 490 in the (S/T)Q context of GLUT1 was identified as an ATM-specific phosphorylation site by LC-MS/MS analysis (Fig. 3a), which is a highly conserved consensus sequence across human, mouse, rat, sheep and chickens (Fig. 3b). Using immunoprecipitation with an antibody specifically recognizing the ATM/ATR substrate of p(S/T-Q) followed by western blotting with antibody against GLUT1 in the immunoprecitated proteins, we detected a decreased signal of endogenous phosphorylated GLUT1 in response to ATM inhibition and ATM knockdown in hypoxic CAFs (Fig. 3c). A phospho-specific antibody against GLUT1 S490 (pGLUT1 S490) was further used to detect p-GLUT1 in CAFs. As shown in Fig. S3a, the phosphorylated GLUT1 at S490 was significantly induced by hypoxia, then attenuated by KU60019 treatment in CAFs. Similar results were acquired using primary CAFs at the same condition (Fig. S3b). After transfection of ectopic wild-type (WT) or mutant GLUT1 (S490A) into the endogenous GLUT1-silenced CAFs (CAF/*Glut1* KD) (Fig. S3c), enhanced phosphorylated-GLUT1 was detected in hypoxic CAF/ecto-Glut1 WT rather than in hypoxic CAF/ecto-Glut1 S490A (Fig. S3d), indicating GLUT1 is specifically phosphorylated at S490 by hypoxia. To further verify the role of oxidized ATM to phosphorylate GLUT1 at serine 490, in vitro ATM kinase assay was carried out. Oxidized ATM could phosphorylate wild-type GLUT1 but not mutant GLUT1 (S490A) under hypoxia detected by Fluorimetric Kinase Assay (Fig. 3d) and immunoblotting with antibody against phosphorylated GLUT1 (Fig. 3e). Notably, KU60019 abolished the GLUT1 phosphorylation by oxidized ATM (Fig. 3d-3e), supporting a critical role of oxidized ATM in directly phosphorylating GLUT1 in hypoxic breast CAFs.

4. Oxidized ATM induces phosphorylated GLUT1 translocation to cellular membrane and PKM2 up-regulation in CAFs.

To understand whether phosphorylation of GLUT1 can lead to cell membrane translocation of GLUT1, cellular membrane GLUT1 in CAFs were evaluated. Using IF staining, we found more membrane GLUT1 in hypoxic CAFs than in normoxic CAFs (Fig. 4a). ATM inhibitor KU60019 treatment blocked GLUT1 translocation to cell membrane, leading to a cytoplasm accumulation of GLUT1 (Fig. 4a). Using biotin pull-down of surface proteins for immunoblotting detection, we verified that membrane GLUT1 was increased in hypoxic CAFs and KU60019 could decrease GLUT1 translocation to cell membrane (Fig. S3e). We also found that membrane GLUT1 was increased in primary CAFs under hypoxia by using biotin pull-down of surface proteins for immunoblotting detection and the translocation to membrane were blocked with the KU60019 treatment as shown in Fig. S3f. To further confirm whether the phosphorylation of ATM specific (S/T-Q) site in GLUT1 (S490) mediated the cell membrane translocation of GLUT1, engineered CAFs with ectopic wild type (CAF/ecto-WT) and mutant GLUT1 S490A (CAF/ecto-S490A) were established and used in experiments. Hypoxia could stimulate endogenous GLUT1 (Fig. 4a) and ectopic wild-type GLUT1 (Fig. 4b, middle left panel; and Fig. S3g), no mutant GLUT1 S490A (Fig. 4B, middle right panel; Fig. S3g) translocated to cell membrane. KU60019 treatment abolished GLUT1 translocation to cell membrane (Fig. 4b, down panel), suggesting phosphorylation of serine 490 is essential for GLUT1 membrane translocation. Accordingly,

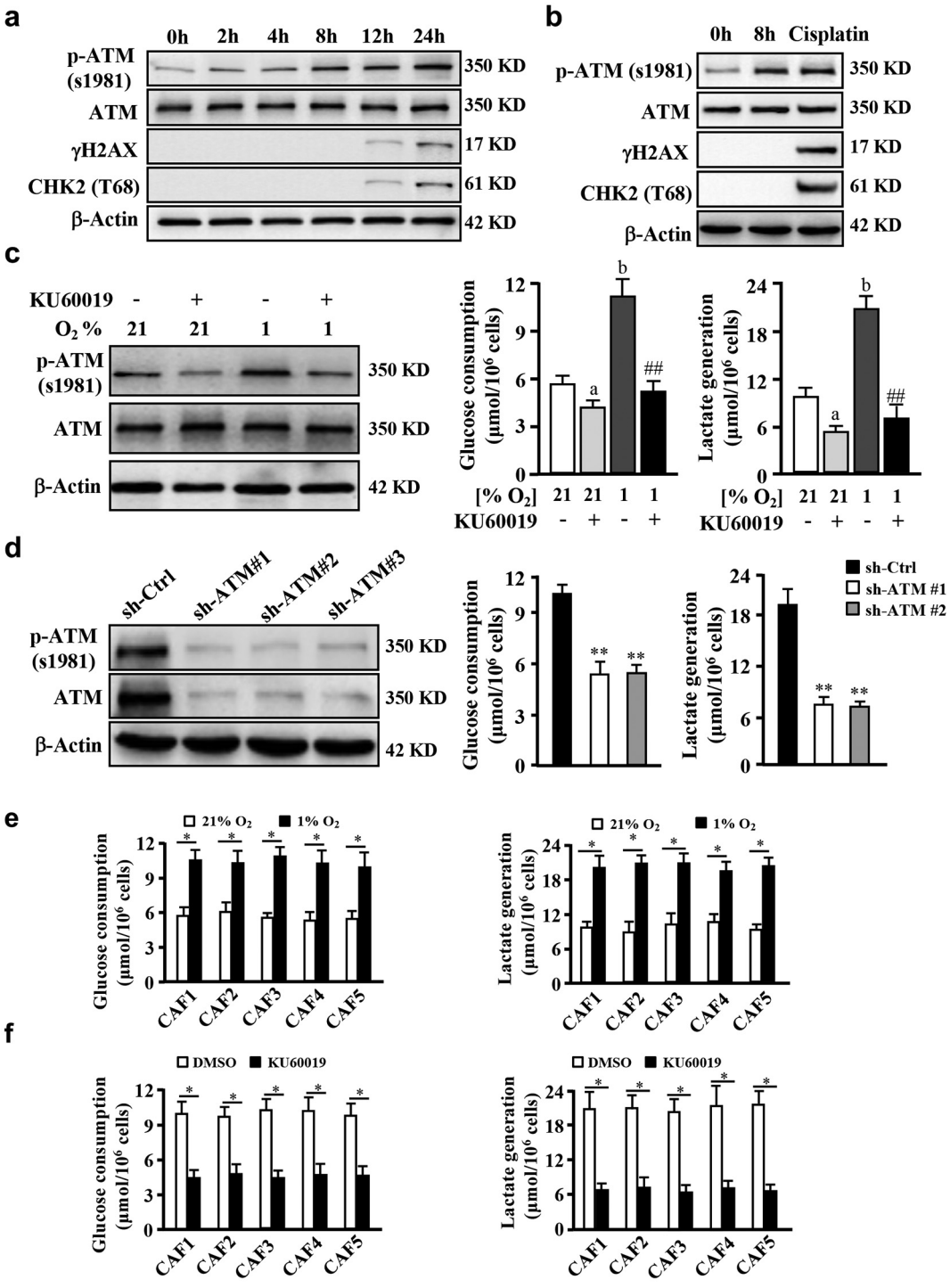

Fig. 2. Hypoxia enhances glycolysis and hypoxia-induced activation of oxidized ATM in CAFs. a. CAFs were cultured in 1% O_2 condition for designed time, western blots showing p-ATM (S1981), ATM, γ-H2AX and CHK2 (T68) levels. β-Actin is the loading control. b. Western blots of p-ATM (S1981), ATM, γ-H2AX and CHK2 (T68) levels in CAFs with different treatment (1% O_2 for 0 h, 1% O_2 for 8 h, 10 μM of cisplatin for 4 h). β-Actin is the loading control. c. CAFs were cultured under 21% O_2 or 1% O_2 for 8 h with or without KU60019 treatment (5 μM). Western blots show levels of p-ATM (S1981), ATM, and β-Actin in CAFs. Glucose consumption and lactate production were detected in same time ([a], $p < .05$, normoxic CAF under KU60019 vs control CAF $p < .01$; [b], $p < .01$, hypoxic CAFs vs normoxic CAFs; [##], $p < .01$, hypoxic CAFs under KU60019 vs hypoxic control CAFs. ANOVA). d. Western blots showing p-ATM (S1981) and ATM proteins in CAFs with three different shRNAs against ATM. Cellular glucose consumption and lactate production were determined in hypoxic CAFs with under depletion of ATM by specific shRNAs against ATM (**, $P < .01$, CAF/shATM vs CAF/shCtrl, Student's *t*-test). e. Five groups of primary CAFs were cultured in normoxia (21% O_2) or hypoxia (1% O_2) for 8 h, the glucose consumption and lactate generation were detected (*, $p < .05$, hypoxic CAFs vs normoxic CAFs, Student's *t*-test). f. Primary CAFs were cultured with or without KU60019 (5 μM) under hypoxia (1% O_2) for 8 h, the glucose consumption and lactate generation were determined (*, $p < .01$, hypoxic CAFs with KU60019 vs hypoxic CAFs with DMSO, Student's *t*-test).

membrane translocation of wild type GLUT1, rather than mutant GLUT1 S490A, caused higher glucose consumption and lactate generation in CAFs, which could be reduced by KU60019 (Fig. 4c). In addition, mutant GLUT1 S490A did not translocate to cell membrane in CAFs under normoxic and hypoxic conditions, and had no effects on glycolytic alteration in CAFs (Fig. 4c). These data indicate that oxidized ATM induces phosphorylation and translocation of GLUT1 in CAFs, thereby increased glycolytic activity of CAFs.

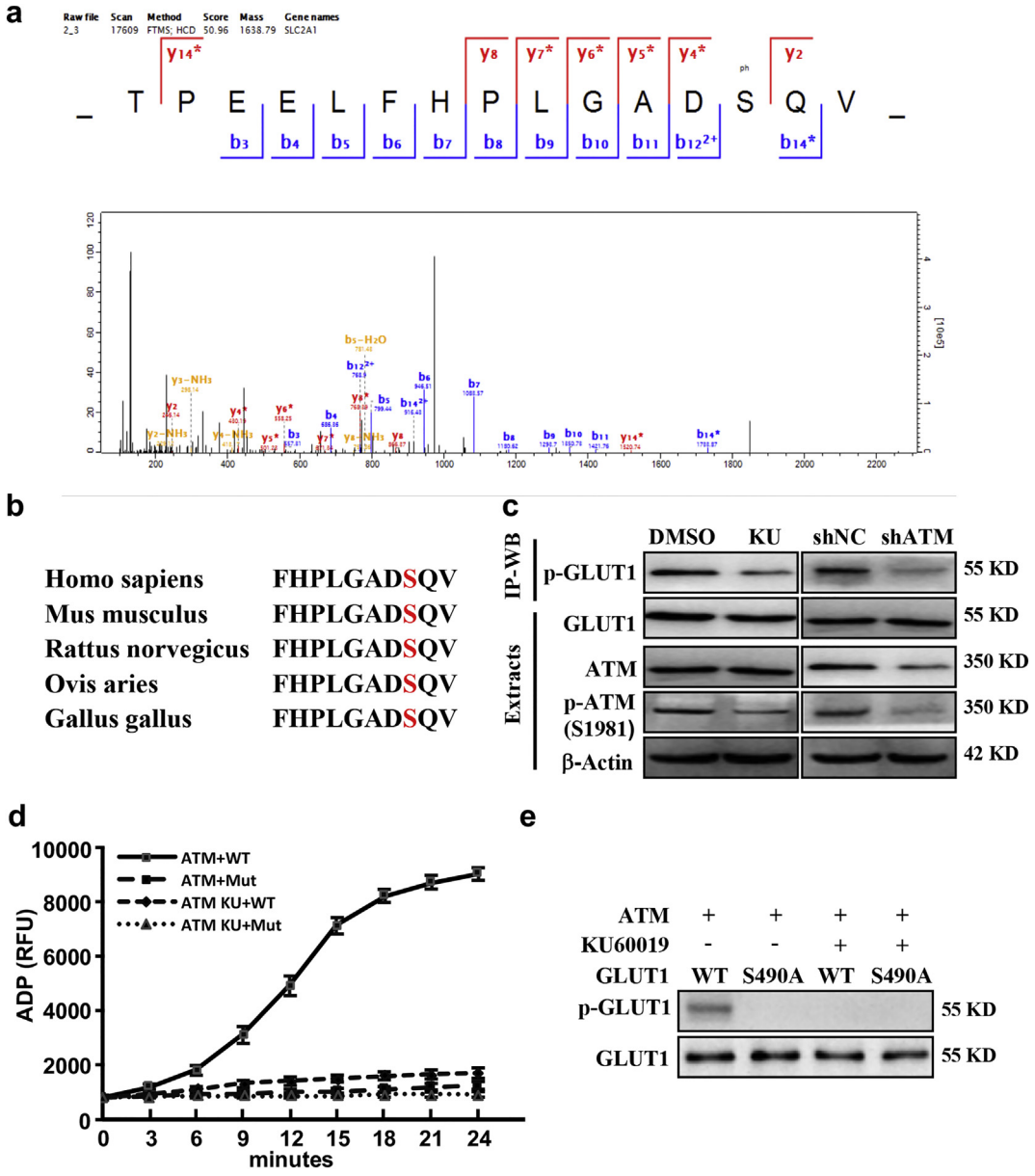

Fig. 3. GLUT1 is a phosphorylated target of oxidized ATM kinase. a. The phosphorylated serine 490 residue in GLUT1 was identified by LC-MS/MS. b. The conserved consensus of ATM phosphorylation site in GLUT1 (Serine 490) of human and other species. c. Cell lysate from CAFs treated with or without KU60019 (labeled with KU) and ATM knocked down-CAFs were immunoprecipitated, the phosphorylated GLUT1 was detected. Protein levels of p-ATM and ATM in cell extracts were detected by western blotting. d. HEK293T cells were transfected with pcDNA3-Flag-ATM or pcDNA3-Flag-GLUT1 WT or mutant (S490A) construct, respectively. Cells with pcDNA3-Flag-ATM were cultured under hypoxia with or without KU60019 (5 μM). In vitro kinase assay was performed using purified ATM kinase mixed with substrates of purified GLUT1. The ADP products (d) and the phosphorylated GLUT1 (e) are shown.

PKM2 plays a pivotal role in cellular glycolysis [30]. As aforementioned, enhanced PKM2 existed in CAFs compared with NFs (see Fig. 1a). To understand whether oxidized ATM could also up-regulate PKM2 expression, we detected PKM2 protein levels in immortalized CAFs and primary CAFs by western blotting. As expected, high levels of PKM2 proteins were detected in hypoxic CAFs than in normoxic CAFs, which was associated with activated AKT (Fig. 4d, and Fig. S3h). Blockage of oxidized ATM activation using KU60019 resulted in decrease of phosphorylated AKT and PKM2 protein levels (Fig. 4d, and Fig. S3h). PKM2 and p-AKT proteins were also reduced by ATM knockdown in hypoxic CAFs (Fig. 4e and f), suggesting that oxidized ATM and its downstream PI3K-AKT signaling regulate PKM2 expression. These date demonstrate that oxidized ATM-mediated cell membrane translocation of phosphorylated GLUT1 and high level of PKM2 in CAFs are critical for glycolysis change in response to hypoxia.

5. Increased glycolytic activity in CAFs fuels breast cancer cell invasion through lactate.

The previous studies unraveled that CAFs can promote cancer cell migration and invasion through secreting proteins and extracellular matrix remodeling [25,31]. We asked whether oxidized ATM-induced glycolysis enhancement in CAFs has an effect on breast tumor cell invasion. Interestingly, breast cancer cells, MDA-MB-231 and BT-549, co-cultured with CM from ATM-knocked down CAFs (CAF/sh-ATM) had a reduced migration (Fig. 5a) or invasion (Fig. 5b) ability in comparison with breast cancer cells co-cultured with CM from control CAFs (CAF/sh-Ctrl). Exogenous lactate added into the supernatant from ATM-silenced CAFs (CAF/sh-ATM) effectively rescued the invasion abilities of breast cancer cells (Fig. 5c). Subsequently, we wondered whether membrane translocation of phosphorylated

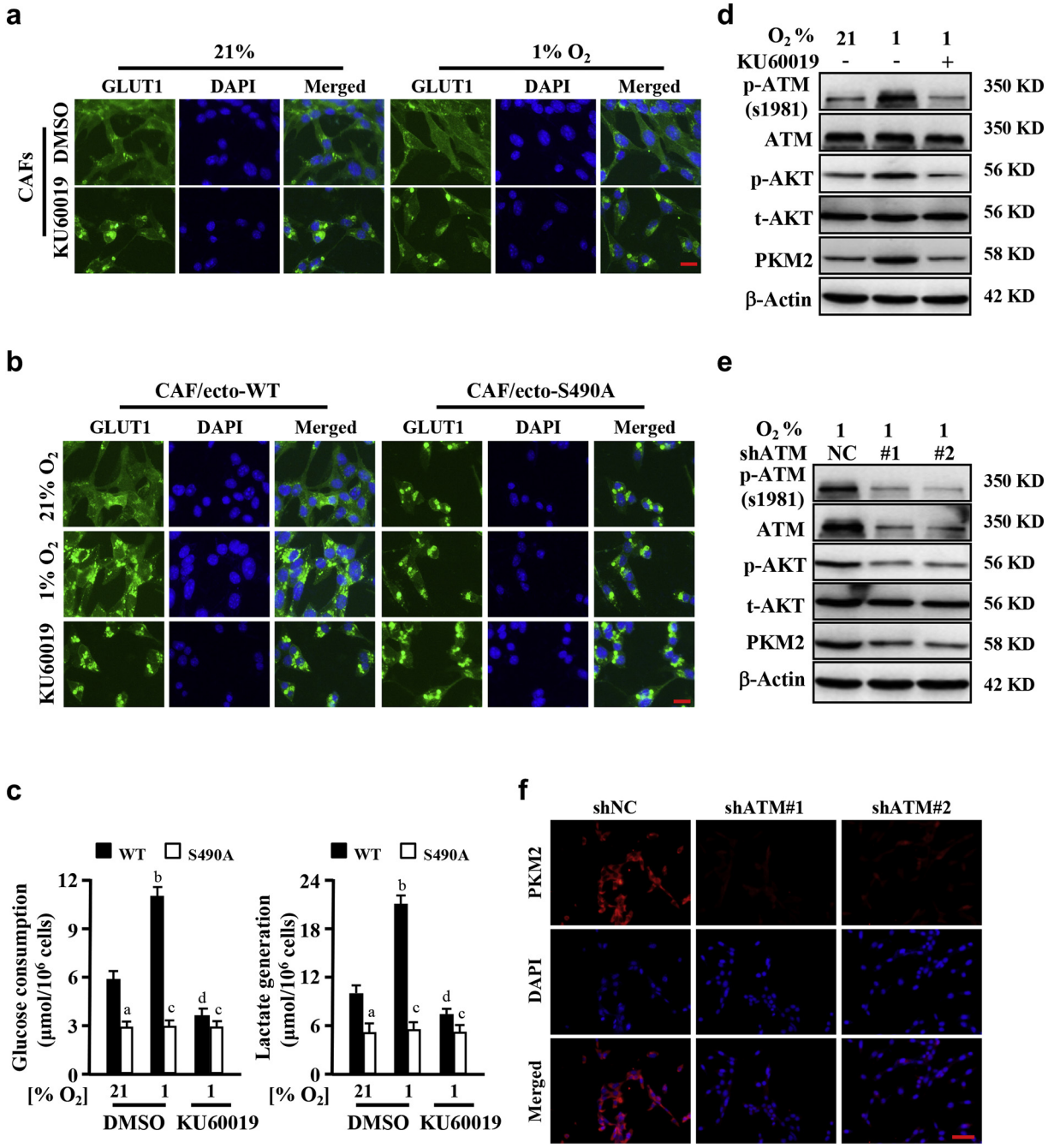

Fig. 4. ATM promotes GLUT1 translocation and PKM2 activation in CAFs. a. CAFs were cultured in normoxia or hypoxia for 8 h and treated with or without KU60019 (5 μM), the membrane GLUT1 was shown by immunofluorescence staining. Scale bar, 50 μm. b. The engineered CAFs (CAF/ecto-WT and CAF/ecto-S490A) (as described at material and methods) were cultured in normoxic or hypoxic condition for 8 h and treated with or without KU60019 (5 μM), the membrane location of GLUT1 in CAFs was detected by immunofluorescence staining. Scale bar, 50 μm. c. Glucose consumption and lactate production of CAFs described in (b) and their parent CAFs were detected. ([a], $p < .01$, normoxic CAF/ecto-S490A vs normoxic CAF/ecto-WT under DMSO treatment; [b], $p < .01$, hypoxic CAF/ecto-WT vs normoxic CAF/ecto-WT; [c], $p > .05$, hypoxic CAF/ecto-S490A vs normoxic CAF/ecto-S490A; [d], $p < .01$, hypoxic CAF/ecto-WT under KU60019 vs DMSO. ANOVA). d. CAFs were cultured in normoxia or hypoxia for 8 h and treated with or without KU60019 (5 μM), protein levels of p-ATM, ATM, p-AKT, AKT and PKM2 were determined by Western blotting. e. Western blotting was used to measure the expressions of p-ATM, ATM, p-AKT, AKT and PKM2 in control CAFs (CAF/sh-NC) and CAFs with shRNAs targeting ATM (CAFs/shATM#1 and CAFs/shATM#2) under hypoxic condition. β-Actin is the loading control in (D) and (E). f. Immunofluorescence staining of PKM2 in CAFs as described in (e). DAPI is specifically dyed for nucleus. Scale bar, 100 μm.

GLUT1 or PKM2 upregulation-mediated lactate generation in hypoxic CAFs directly contribute to breast tumor cell invasion. Indeed, CM from hypoxic CAF/ecto-S490A hampered the invasive abilities of MDA-MB-231 and BT-549 cells in contrast to CM from hypoxic CAF/ecto-WT (Fig. S4a). Similar data were acquired from PKM2 wild-type and PKM2-knocked down CAFs, in which loss of PKM2 led to lactate decrease(Fig. S4b) and reduced breast tumor cell invasion (Fig. S4c).

To further confirm these findings, MCT4 (the main exporter of lactate in stromal fibroblasts) or MCT1 (the key monocarboxylate transporter for uptake of lactate into tumor cells) [4] was knocked down by shRNA in CAFs or in tumor cells, respectively. As expected, knockdown of MCT4 in hypoxic CAFs led to reduced lactate in supernatant (Fig. S4d), thus decreased tumor cell invasion in the co-culture system (Fig. 5d); Loss of MCT1 in MDA-MB-231 and BT-549 cells decreased lactate uptake from CM of hypoxic CAFs (Fig. S4e) and yielded an

attenuated tumor cell invasion (Fig. 5e). Taken together, these data suggest that oxidized ATM-mediated glycolysis enhancement in CAFs facilitates tumor cell invasion through lactate from fibroblasts.

6. Lactate derived from hypoxic CAFs promotes cancer cell invasion by triggering TGFβ1/p38 MAPK/MMP2/9 signaling and increasing mitochondrial activity.

It has been reported that lactate can activate signaling cascades, such as TGFβ2 signaling in glioma [32], indicating lactate works as an energy metabolic coupling between CAFs and tumor cells to trigger downstream pathways in fueling tumor cell invasion. Of note, high levels of TGFβ1, phosphorylated P38 (p-P38), MMP2, and MMP9 were detected in MDA-MB-231 and BT-549 cells co-cultured with CM from hypoxic CAFs, and knockdown of ATM by specific shRNA decreased these protein levels (Fig. 6a), indicating CM from hypoxic CAFs could stimulate TGFβ1/p38 MAPK/MMP2/9 signaling in MDA-MB-231 and BT549 breast cancer cells. Addition of lactate to MDA-MB-231 and BT-549 cells increased the activation of TGFβ1/p38 MAPK/MMP2/9 signaling (Fig. 6b). Co-culture of tumor cells in CM from CAFs/ecto-S490A resulted in reduced TGFβ1, p-P38, MMP2 and MMP9 proteins in tumor cells (Fig. 6c). In line with these findings, the protein levels in tumor cells were decreased by the CM from CAFs/sh-PKM2 (Fig. 6d). Furthermore, silencing MCT4 in hypoxic CAFs (Fig. 6e) or knockdown of MCT1 in tumor cells (Fig. 6f), which blocks lactate transport into tumor cells, led to attenuated activation of this signaling cascade. These data reveal a lactate-dependent TGFβ1/p38 MAPK/MMP2/9 signaling axis involved in breast tumor cell invasion.

On the other hand, lactate can serve as an energy supply to fuel mitochondria metabolism [33]. Indeed, co-culture of breast tumor cells MDA-MB-231 and BT-549 with CM from ATM-knocked down CAFs (CAF/sh-ATM), the OxPhos OCR in tumor cells were reduced (Fig. S5a). Supplementation of exogenous lactate (20 mM) in the CM from CAF/sh-ATM could rescue mitochondrial activities of tumor cells (Fig. S5b), indicating that hypoxic CAFs-derived lactate activates mitochondrial activity in tumor cells. To confirm whether the enhanced mitochondrial activity stimulated by hypoxic CAFs-derived lactate was associated with cancer cell invasion, oligomycin, an anti-mitochondrial drug reported in previous study [34] was used in our experiments. After the treatment of oligomycin, the reduced mitochondrial activity in MDA-MB-231 and BT-549 cells were reflected by declined OxPhos OCR (Fig. S5c, Fig. S5e), and the invasion ability of cancer cells was decreased correspondingly (Fig. S5d, Fig. S5f). In summary, theses data show that hypoxic CAFs-derived lactate may also accelerate cancer cell invasion through fueling mitochondrial activity of tumor cells.

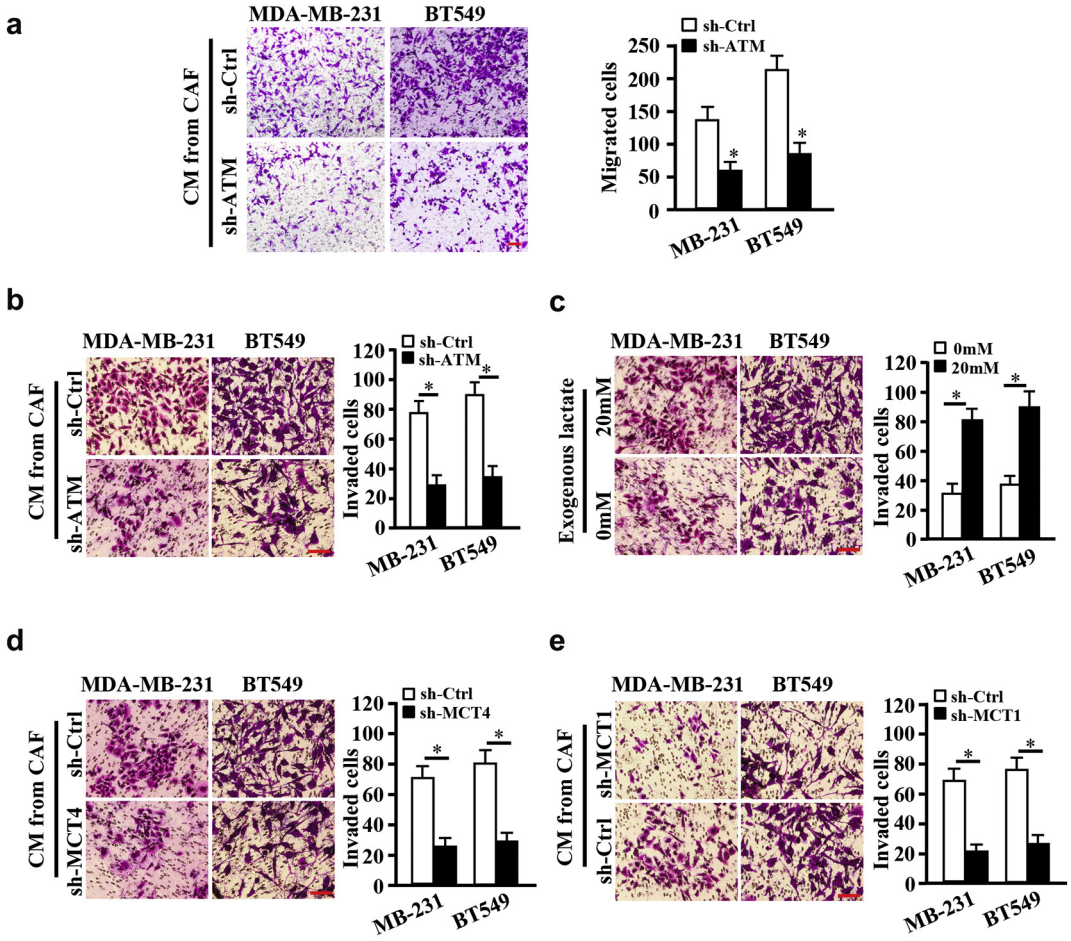

Fig. 5. CAFs enhance migration and invasion of breast cancer cells through glycolysis. a. Breast cancer cells BT549 and MDA-MB-231 (or labeled as MB-231) were cocultured with CM from control CAFs (CAFs/sh-Ctrl) or ATM-silenced CAFs (CAFs/sh-ATM). Cellular migration ability was detected by Transwell assay (without ECM coated). The average migrated cells were showed by histograms (*, $P < .01$, Student's *t*-test). b-e. Breast cancer cells of BT549 and MDA-MB-231 (or labeled as MB-231) were seeded into the Boyden chambers (coated with ECM) and co-cultured with CM from different hypoxic CAFs, cell invasion abilities were measured. b. Breast cancer cells were mixed with CM from ATM-knocked down or control CAFs. c. Breast cancer cells were co-cultured with CM from hypoxic CAF/sh-ATM added with or without exogenous lactate (20 mM). d. Breast cancer cells were mixed with CM from the hypoxic CAFs transfected with specific shRNA against MCT4 or control shRNA. e. Breast cancer cells transfected with specific shRNA against MCT1 or control shRNA were cultured in the CM from hypoxic CAFs. The histograms show the average invaded cells each view (*, $P < .01$, Student's *t*-test). Scale bar, 100 μm.

7. Oxidized ATM-mediated lactate accumulation through glycolysis in CAFs promotes breast tumor metastasis in vivo.

To confirm hypoxic CAFs-derived lactate induced by oxidized ATM-mediated glycolytic enhancement to fuel tumor metastasis, MDA-MB-231 cells mixed with the CAFs, or engineered CAFs (CAF/sh-ATM, CAF/sh-MCT4) were subcutaneously transplanted into nude mice. Compared with the tumor burden mice injected with mixture of MDA-MB-231 and control CAFs, the tumor burden mice which injected with MDA-MB-231 and engineered CAFs (CAF/sh-ATM, CAF/sh-MCT4) had a significant small tumor (Fig. 7a; Fig. S6a-S6b) and fewer lung metastases (Fig. 7b, and Fig. S6c-S6d); application of 2-deoxyglucose (2-DG, a non-metabolized glucose analogue) or CHC (CAF/sh-Ctrl/CHC) to the tumor burden mice, injected with MDA-MB-231 and control CAFs, also decreased tumor growth (Fig. 7a; Fig. S6a-S6b) and correspondingly reduced metastases in mice lung tissues (Fig. 7b; Fig. S6c-S6d). In contrast, supplementation of exogenous lactate to the mice injected with MDA-MB-231 and ATM-knocked down CAFs (CAF/sh-ATM) could partially rescue tumor growth or metastasis (Fig. 7a-7b, and Fig. S6c-S6d). Blockage of

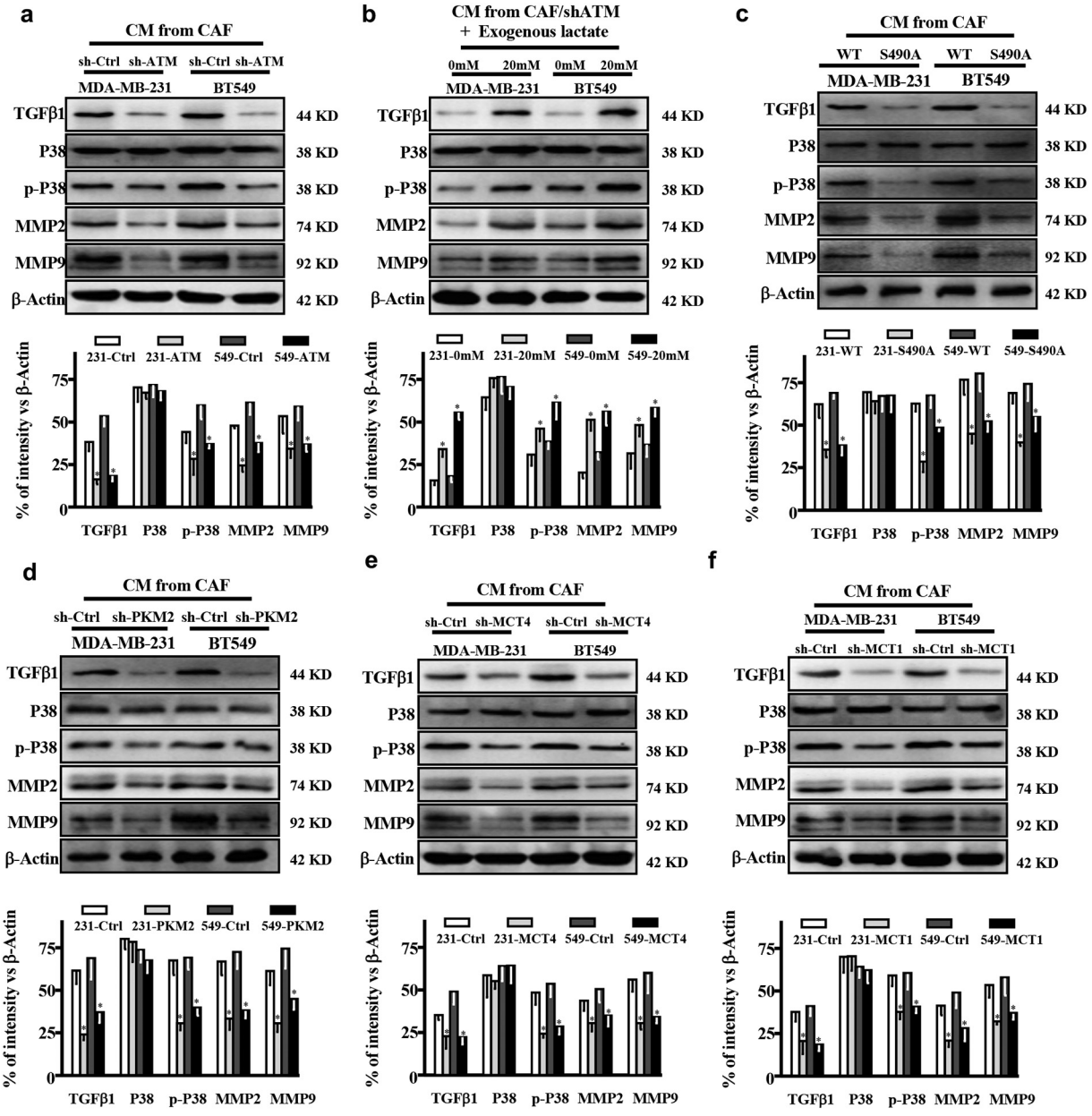

Fig. 6. Lactate derived from CAFs activates TGFβ1/p38 MAPK/MMP2/9 signaling in breast cancer cells. a. The indicated breast cancer cells co-cultured with supernatant derived from control CAFs (CAFs/sh-Ctrl) or ATM-silenced CAFs (CAFs/sh-ATM), protein levels of TGF-β1, total P38, p-P38, MMP2, and MMP9 in MDA-MB-231 and BT-549 cells were determined by Western blotting. b. CM from ATM-silenced CAFs (CAF/sh-ATM) with or without exogenous lactate (20 mM) was used to culture with breast cancer cells, the expressions of TGFβ1, P38, p-P38, MMP2, and MMP9 in MDA-MB-231 and BT-549 cells were detected by Western blotting. c-d. Expressions of TGFβ1, P38, p-P38, MMP2 and MMP9 in MDA-MB-231 and BT-549 cells were determined by Western blotting under co-culture with CM from the endogenous GLUT1 silenced CAFs re-transfected with WT (CAF/WT), or mutant GLUT1 S490A (CAF/S490A) (c); CAFs transfected with control shRNA (CAF/sh-Ctrl) or sh-PKM2 (CAF/sh-PKM2) (d).e. MDA-MB-231 and BT-549 were co-cultured with supernatant from CAFs transfected with control shRNA or specific shRNA against MCT4. The expressions of TGFβ1, P38, p-P38, MMP2, and MMP9 were determined using Western blotting. f. MDA-MB-231 and BT-549 cells transfected with control shRNA or specific shRNA against MCT1 were co-cultured with supernatant from CAF. Western blotting was done to detect the expressions of TGFβ1, P38, p-P38, MMP2, and MMP9 in MDA-MB-231 and BT-549. β-Actin was used as a loading control for Western blotting assay. The histograms of densitometric analysis were shown accompanied with western blots respectively (*, $P < .05$, Student's *t*-test).

glycolysis or inhibition of the lactate coupling between CAFs and tumor cells led to reduction of TGFβ1/p38 MAPK signaling (Fig. 7c), thus decreased MMP2, MMP9 and TGFβ1 expressions (Fig. 7c-7d and Fig. S6e). Administrating the mice injected with MDA-MB-231 and ATM-knocked down CAFs using exogenous lactate could partially rescue the TGFβ1/p38 MAPK signaling, and increased MMP2, MMP9 and TGFβ1 levels in tumor tissues (Fig. 7c-7d, and Fig. S6e). These data support that oxidized ATM-mediated glycolysis in CAFs can promote breast cancer cell invasion and metastasis through lactate transfer between CAFs and cancer cells.

4. Discussion

Oxidative phosphorylation (OxPhos) is the predominant ATP supplier and supports tumor growth in several cancer cell types [34,35]. However, hypoxia is one of typical features in tumor tissues because of accelerated proliferation and poorly angiogenesis [36,37]. Hypoxia exerts a profound influence on tumor biology and regulates the hallmarks of cancer cells (such as stemness, metabolic reprogramming, resistance to anticancer therapies). Besides, hypoxia is highly related with tumor aggressiveness and poor prognosis [38]. In our previous study,

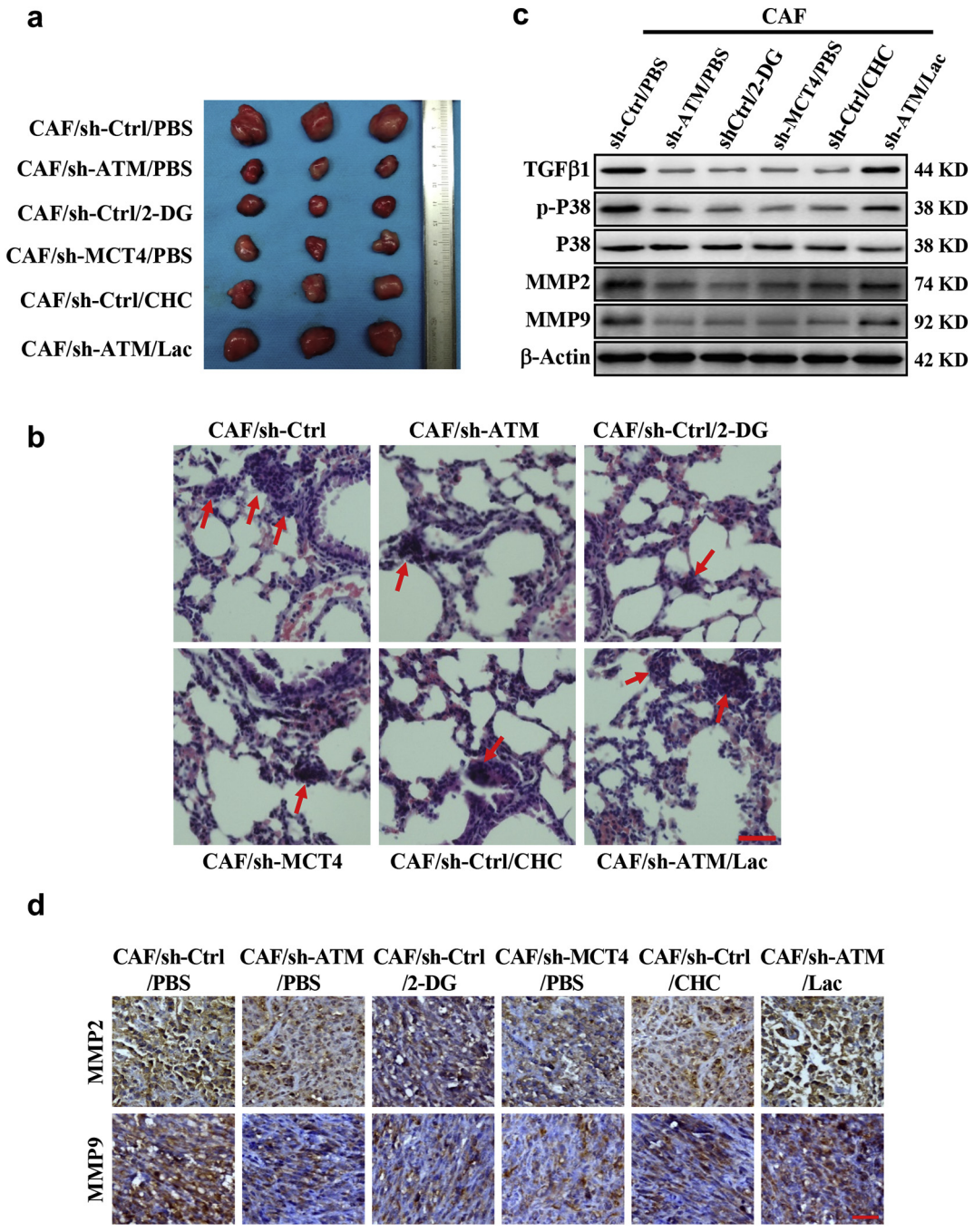

Fig. 7. ATM-induced glycolysis is required for CAF-facilitated mammary tumor metastasis in mice. Breast cancer cell MDA-MB-231 mixed with the CAFs or engineered CAFs (CAF/sh-ATM, CAF/sh-MCT4) were subcutaneously transplanted into nude mice. The mice were treated with 2-DG, CHC or lactate as described in materials. a. The tumor size in mice. b. The representative images of pulmonary metastases checked by H&*E*-staining; the red arrows showing the metastases; Scale bar, 40 μm. c. Protein levels of TGF-β1, total and phosphorylated P38, MMP2 and MMP9 in tumor tissues were detected by Western blotting. d. Representative images of MMP2 and MMP9 examined by IHC staining are shown; Scale bar, 40 μm.

we found hypoxia can enhance the proliferation of breast CAFs. To survive in hypoxic condition, the cells in tumor tissues tend to glycolysis more than pyruvate metabolism and oxidative phosphorylation [39]. In this study, we reveal a crucial mechanism underlying the oxidized ATM-induced glycolysis alterations in stromal CAFs. Compared with NFs, the oxidized ATM protein is enhanced in breast CAFs, companied with lower OCR and higher ECAR. In addition, weaker mitochondrial membrane potential and less mitochondrial were detected in CAFs. Hypoxia-stimulated oxidized ATM promotes the glycolysis phenotype in a DSB-independent manner in CAFs. Metabolites lactate derived from CAFs act as a metabolic coupling link between CAFs and breast tumor cells to trigger the downstream TGFβ1/p38 MAPK/MMP2/9 signaling and increase mitochondrial activity in tumor cells, thus fueling tumor cell invasion. Our works demonstrate that the oxidized ATM plays a key role in glycolysis process in breast CAFs and promotes tumor invasion through lactate-mediated metabolic coupling.

Oxidized ATM exists in breast CAFs compared to NFs. Traditionally, ATM has been activated via DSBs and performs the DSB repair response through phosphorylating downstream substrates such as γH2AX, a biomarker of the DSB-dependent ATM activation [40]. Recently, some of evidence suggests that ATM protein kinase can be enabled directly by oxidative stress in cytoplasm, which is independence of the canonical DSB-induced ATM activation mechanism [13]. Generally, the cellular ROS levels, which are closely associated with hypoxia, are important to maintain cellular redox homeostasis [41]. The high levels of cellular ROS can stimulate auto-phosphorylation of ATM at Ser1981, a hallmark of the activation of the oxidized ATM kinase [42]. Application of NAC (antioxidant) to CAFs specifically decrease the ROS amount and reduce the p-ATM (s1981) protein levels in CAFs, indicating that the oxidized ATM kinase may be activated by ROS in hypoxic breast CAFs.

Oxidized ATM can promote glycolysis in breast CAFs. A growing number of studies have provided converging evidence for oxidized ATM in the absence of DSBs participating in other cell biological process. For example, oxidized ATM phosphorylates distinct substrates such as HIF1α at Ser696, leading to the specific activation of HIF1α signaling [43]. The oxidized ATM plays a critical role in breast CAF cell proliferation by activating the PI3K-AKT, MEK-ERK, and Wnt/β-catenin signaling pathways [11]. In addition, oxidized ATM promotes cell glucose absorption in muscle cells, indicating that oxidized ATM is a regulator of cellular energy metabolism [14]. GLUT1 has been found to take charge in the Warburg effect in some human tumor cells [44]. Especially, the carboxy terminal of GLUT1 plays key roles in the biological function of GLUT1 [45]. We showed that hypoxia-induced oxidized ATM plays a positive role in the glycolysis enhancement of breast CAFs by directly phosphorylating GLUT1 at Ser490, the specific ATM-phosphorylated (S/T)Q motif which locates at the C-terminal of GLUT1 [46], and up-regulating PKM2 expression through PI3K/AKT signaling. Here, phosphorylation of GLUT1 at Ser490 by the oxidized ATM results in the translocation of GLUT1 to the plasma membrane and is responsible for the increased glucose uptake in CAFs. Our data demonstrate that hypoxia-induced ATM protein kinase plays a direct role in GLUT1 phosphorylation and plasma membrane translocation, thus promoting the glycolysis enhancement in CAFs. In addition, oxidized ATM also up-regulating PKM2 expression through PI3K/AKT signaling. PKM2 promotes pyruvate production and ATP generation in the glycolytic pathway. For example, PKM2 expression contributes to aerobic glycolysis of cancer cells for tumor growth [47]. In vitro, overexpression of Twist in breast cancer cells results in Warburg effect through elevation of PKM2 via activating integrin β1-FAK-PI3K-AKT-mTOR axis [48]. Here, we show that the expression of PKM2 is enhanced by oxidized ATM via PI3K/AKT signaling and contributes to glycolysis of breast CAFs under hypoxia. Thus, our works demonstrate that oxidized ATM in hypoxic CAFs can induce the robust glycolytic activity through phosphorylating GLUT1 and PI3K/AKT-dependent PKM2 up-regulation.

Furthermore, we unravel that metabolites lactate from CAFs acts as metabolic coupling between CAFs and tumor cells to stimulate up-regulation of MMP2 and MMP9 and motivate the mitochondrial activity to fuel tumor cell invasion. Recently, it has been reported that tumor cells in microenvironment function as metabolic parasites to take up energy (such as L-lactate, ketones, and glutamine, free fatty acids) from surrounding host cells (e.g. fibroblasts and adipocytes) to increase their ability for oxidative phosphorylation (OXPHOS), thus driving tumor cell proliferation, apoptotic resistance [22,49] and drug resistance [26]. We found that the metabolism coupling boosts tumor invasion via lactate shuttle from CAFs, and the lactate from CAFs can be used for the enhanced mitochondrial activity in breast cancer cells. It has been shown that lactate, the product of glycolysis, has significant effects on tumor angiogenesis, tumorigenesis, tumor immune escape and self-sufficient metabolism [50,51]. However, only a few of studies have identified the key elements or specific signaling of lactate-induced tumor cell biological behavior alteration. For instance, the metabolic intermediate lactate could act as a signaling molecule activator to the autocrine NF-κB/IL-8 pathway to promote angiogenesis in tumors [52]. Angiogenesis can also be promoted directly by lactate engaging three RTKs signaling in cancer [53]. Our data demonstrate that the CAF-derived lactate stimulates TGFβ1/p38 MAPK-dependent up-regulation of MMP2 and MMP9, thus contributing to tumor cell invasion.

In conclusion, oxidized ATM-mediated enhanced glycolysis in breast CAFs. The oxidization and activation of ATM in hypoxia can promote both GLUT1-phosphorylation and PKM2 up-regulation to facilitate lactate production. Lactate, as a metabolic coupling mediator between CAFs (released by MCT4) and tumor cells (absorbed via MCT1), promotes tumor cell invasion through activation of TGFβ1/p38 MAPK/MMP2/9 signaling and fueling the mitochondrial activity in tumor cells. Thus, our work highlights a novel mechanism by which stromal fibroblasts fuel tumor invasion and may implicate a new strategy for breast cancer therapy.

Funding

This work was supported in part by National Natural Science Foundation of China (NSFC 81472476, NSFC 31171336, NSFC 31671481, NSFC 81072147) for Manran Liu. It was also partly supported by NSFC 81560430 for Shifu Tang, and by the Outstanding Talent Fund of Chongqing Medical University (BJRC201703) and Chongqing education committee (CYB17113) for Kexin Sun. Xiaojiang Cui is supported by National Institutes of Health (2R01CA151610), Department of Defense (W81XWH-18-1-0067), the Fashion Footwear Charitable Foundation of New York, Inc., and the Margie and Robert E. Petersen Foundation. We have not been paid to write this article by any pharmaceutical company or other agency. The funding role had no role in study design, data collection, data analysis, interpretation, writing of the report.

Author contributions

K.S. and S.T. carried out most of experiments, Y.H. and L.X. provided primary fibroblasts and contributed to the experimental design. J.Y., M.P., and M.Z. performed cell culture. D.Y. contributed to the data analysis. L.X. and Y.C. performed the bioinformatic analysis. M.L. and X.C. conceived and designed experiments and wrote the manuscript. All authors read and approved the manuscript. The corresponding author have full access to all the data in the study and have final responsibility for the decision to submit for publication.

Conflicts of interest

The authors declare no conflict of interest.

Appendix A. Supplementary data

Supplementary data to this article can be found online at https://doi.org/10.1016/j.ebiom.2019.02.025.

References

[1] Tang S, Yang L, Tang X, Liu M. The role of oxidized ATM in the regulation of oxidative stress-induced energy metabolism reprogramming of CAFs. Cancer Lett 2014;353(2):133–44.
[2] Cirri P, Chiarugi P. Cancer associated fibroblasts: the dark side of the coin. Am J Cancer Res 2011;1(4):482–97.
[3] Moreno-Sánchez R, Rodríguez-Enríquez S, Marín-Hernández A, et al. Energy metabolism in tumor cells. FEBS J 2007;274(6):1393–418.
[4] Pavlides S, Whitaker-Menezes D, Castello-Cros R, et al. The reverse Warburg effect: aerobic glycolysis in cancer associated fibroblasts and the tumor stroma. Cell Cycle 2009;8(23):3984–4001.
[5] Guise CP, Mowday AM, Ashoorzadeh A, et al. Bioreductive prodrugs as cancer therapeutics: targeting tumor hypoxia. Chin J Cancer 2014;33(2):80–6.
[6] Narayan V, Iyer NV, Kotch LE, Agani F, et al. Cellular and developmental control of O2 homeostasis by hypoxia-inducible factor 1alpha. Genes Dev 1998;12(2):149–62.
[7] Matsuoka S, Rotman G, Ogawa A. Ataxia telangiectasia-mutated phosphorylates Chk2 in vivo and in vitro. PNAS 2000;97:10389–94.
[8] Kobayashi M, Hirano A, Kumano T, et al. Critical role for chicken Rad17 and Rad9 in the cellular response to DNA damage and stalled DNA replication. Genes Cells 2004;9(4):291–303.
[9] Taira N, Yamamoto H, Yamaguchi T, et al. ATM augments nuclear stabilization of DYRK2 by inhibiting MDM2 in the apoptotic response to DNA damage. J Biol Chem 2010;285(7):4909–19.
[10] Bhoumik A, Takahashi S, Breitweiser W, et al. ATM-dependent phosphorylation of ATF2 is required for the DNA damage response. Mol Cell 2005;18(5):577–87.
[11] Guo Z, Kozlov S, Lavin M, et al. ATM activation by oxidative stress. Science 2010;330(6003):517–21.
[12] Tang S, Hou Y, Zhang H, et al. Oxidized ATM promotes abnormal proliferation of breast CAFs through maintaining intracellular redox homeostasis and activating the PI3K-AKT, MEK-ERK, and Wnt-beta-catenin signaling pathways. Cell Cycle 2015;14(12):1908–24.
[13] Kim J, Wong PK. Oxidative stress is linked to ERK1/2-p16 signaling-mediated growth defect in ATM-deficient astrocytes. J Biol Chem 2009;284(21):14396–404.
[14] Halaby M, Hibma J, He J, et al. ATM protein kinase mediates full activation of Akt and regulates glucose transporter 4 translocation by insulin in muscle cells. Cell Signal 2008;20(8):1555–63.
[15] Armata HL, Golebiowski D, Jung DY, et al. Requirement of the ATM/p53 tumor suppressor pathway for glucose homeostasis. Mol Cell Biol 2010;30(24):5787–94.
[16] Peng Q, Zhao L, Hou Y, et al. Biological characteristics and genetic heterogeneity between carcinoma-associated fibroblasts and their paired normal fibroblasts in human breast cancer. PLoS One 2013;8(4):e60321.
[17] Lopez-Serra P, Marcilla M, Villanueva A, et al. A DERL3-associated defect in the degradation of SLC2A1 mediates the Warburg effect. Nat Commun 2014;5:3608.
[18] Andrisse S, Patel GD, Chen JE, et al. ATM and GLUT1-S490 phosphorylation regulate GLUT1 mediated transport in skeletal muscle. PLoS One 2013;8(6):e66027.
[19] Mazurek S. Pyruvate kinase type M2: a key regulator of the metabolic budget system in tumor cells. Int J Biochem Cell Biol 2011;43:969–80.
[20] David CJ, Chen M, Assanah M, et al. HnRNP proteins controlled by c-Myc deregulate pyruvate kinase mRNA splicing in cancer. Nature 2009;463(7279):364–8.
[21] Discher D, Bishopric N, Wu X, et al. Hypoxia regulates Enolase and pyruvate kinase-M promoters by modulating Sp1/Sp3 binding to a conserved GC element. J Biol Chem 1998;273:26087–93.
[22] Martinez-Outschoorn UE, Lin Z, Whitaker-Menezes D, et al. Ketone body utilization drives tumor growth and metastasis. Cell Cycle 2012;11(21):3964–71.
[23] Ko YH, Lin Z, Flomenberg N, et al. Glutamine fuels a vicious cycle of autophagy in the tumor stroma and oxidative mitochondrial metabolism in epithelial cancer cells: implications for preventing chemotherapy resistance. Cancer Biol Ther 2011;12(12):1085–97.
[24] Lee DC, Sohn HA, Park ZY, et al. A lactate-induced response to hypoxia. Cell 2015;161(3):595–609.
[25] Wang L, Hou Y, Sun Y, et al. C-ski activates cancer-associated fibroblasts to regulate breast cancer cell invasion. Mol Oncol 2013;7(6):1116–28.
[26] Yu T, Yang G, Hou Y, et al. Cytoplasmic GPER translocation in cancer-associated fibroblasts mediates cAMP/PKA/CREB/glycolytic axis to confer tumor cells with multidrug resistance. Oncogene 2017;36(15):2131–45.
[27] Marín-Hernández A, López-Ramírez SY, Del Mazo-Monsalvo I, et al. Modeling cancer glycolysis under hypoglycemia, and the role played by the differential expression of glycolytic isoforms. FEBS J 2014;281(15):3325–45.
[28] Ditch S, Paull T. The ATM protein kinase and cellular redox signaling: beyond the DNA damage response. Cell 2012;37:15–22.
[29] Hruz P, Mueckler M. Structural analysis of the GLUT1 facilitative glucose transporter. Mol Membr Biol 2001;18:183–93.
[30] Christofk HR, Vander Heiden MG, Harris MH, et al. The M2 splice isoform of pyruvate kinase is important for cancer metabolism and tumour growth. Nature 2008;452(7184):230–3.
[31] Tang X, Hou Y, Yang G, et al. Stromal miR-200s contribute to breast cancer cell invasion through CAF activation and ECM remodeling. Cell Death Differ 2016;23(1):132–45.
[32] Baumann F, Leukel P, Doerfelt A, et al. Lactate promotes glioma migration by TGF-b2–dependent regulation of matrix metalloproteinase-2. Neuro Oncol 2009;11(4):368–81.
[33] Ubaldo EM, Michael PL, Federica S. Catabolic cancer-associated fibroblasts (CAFs) transfer energy and biomass to anabolic cancer cells, fueling tumor growth. Semin Cancer Biol 2014;25:47–60.
[34] Mandujano-Tinoco EA, Gallardo-Pérez JC, Marín-Hernández A, et al. Anti-mitochondrial therapy in human breast cancer multi-cellular spheroids. Biochim Biophys Acta 2013;1833(3):541–51.
[35] Rodríguez-Enríquez S, Hernández-Esquivel L, Marín-Hernández A, et al. Mitochondrial free fatty acid β-oxidation supports oxidative phosphorylation and proliferation in cancer cells. Int J Biochem Cell Biol 2015;65:209–21.
[36] Sonveaux P, Vegran F, Schroeder T, et al. Targeting lactate-fueled respiration selectively kills hypoxic tumor cells in mice. J Clin Invest 2008;118(12):3930–42.
[37] Marín-Hernández Á, Gallardo-Pérez JC, Hernández-Reséndiz I, et al. Hypoglycemia enhances epithelial-mesenchymal transition and invasiveness, and restrains the Warburg phenotype, in hypoxic HeLa cell cultures and microspheroids. J Cell Physiol 2017;232(6):1346–59.
[38] Qiu GZ, Jin MZ, Dai JX, et al. Reprogramming of the tumor in the hypoxic niche: the emerging concept and associated therapeutic strategies. Trends Pharmacol Sci 2017;38(8):669–86.
[39] Gatenby RA, Gillies RJ. Why do cancers have high aerobic glycolysis? Nat Rev Cancer 2004;4(11):891–9.
[40] Lee JH, Paull TT. Direct activation of the ATM protein kinase by the Mre11/Rad50/Nbs1 complex. Science 2004;304:93–6.
[41] Ray PD, Huang BW, Tsuji Y. Reactive oxygen species (ROS) homeostasis and redox regulation in cellular signaling. Cell Signal 2012;24(5):981–90.
[42] Bencokova Z, Kaufmann MR, Pires IM, et al. ATM activation and signaling under hypoxic conditions. Mol Cell Biol 2009;29(2):526–37.
[43] Cam H, Easton JB, High A, Houghton PJ. mTORC1 signaling under hypoxic conditions is controlled by ATM-dependent phosphorylation of HIF-1alpha. Mol Cell 2010;40(4):509–20.
[44] Hamanaka RB, Chandel NS. Targeting glucose metabolism for cancer therapy. J Exp Med 2012;209(2):211–5.
[45] Dauterive R, Laroux S, Bunn RC, et al. C-terminal mutations that Alter the turnover number for 3-O-Methylglucose transport by GLUT1 and GLUT4. J Biol Chem 1996;271:11414–21.
[46] Matsuoka S, Ballif BA, Smogorzewska A, et al. ATM and ATR substrate analysis reveals extensive protein networks responsive to DNA damage. Science 2007;316(5828):1160–6.
[47] Luo W, Semenza GL. Emerging roles of PKM2 in cell metabolism and cancer progression. Trends Endocrinol Metab 2012;23(11):560–6.
[48] Yang L, Hou Y, Yuan J, et al. Twist promotes reprogramming of glucose metabolism in breast cancer cells through PI3K/AKT and p53 signaling pathways. Oncotarget 2015;6(28):25755–69.
[49] Nieman KM, Kenny HA, Penicka CV, et al. Adipocytes promote ovarian cancer metastasis and provide energy for rapid tumor growth. Nat Med 2011;17(11):1498–503.
[50] Doherty JR, Cleveland JL. Targeting lactate metabolism for cancer therapeutics. J Clin Invest 2013;123(9):3685–92.
[51] Millán IS, Brooks GA. Reexamining cancer metabolism: lactate production for carcinogenesis could be the purpose and explanation of the Warburg effect. Carcinogenesis 2016;38(2):119–33.
[52] Vegran F, Boidot R, Michiels C, et al. Lactate influx through the endothelial cell monocarboxylate transporter MCT1 supports an NF-kappaB/IL-8 pathway that drives tumor angiogenesis. Cancer Res 2011;71(7):2550–60.
[53] Ruan G, Kazlauskas Andrius. Lactate engages receptor tyrosine kinases Axl, Tie2, and vascular endothelial growth factor receptor 2 to activate Phosphoinositide 3-kinase/Akt and promote angiogenesis. J Biol Chem 2013;288(29):21161–72.